ENCIT 2018

ABCM Associação Brasileira de Engenharia e Ciências Mecânicas

17th Brazilian Congress of Thermal Sciences and Engineering
November 25th-28th, 2018, Águas de Lindóia, SP, Brazil

ENCIT-2018-0439
Stability of Binary Mixing Layers Under the Effect of Buoyancy Forces

Yan da Silva Pedroni [1]
Fernando Fachini Filho [2]
Group of Reactive Fluid Mechanics
INPE - Instituto Nacional de Pesquisas Espaciais, Cachoeira Paulista, SP, Brazil
[1]yanpedroni@gmail.com, [2]fachini@lcp.inpe.br

Marcio Teixeira de Mendonca
IAE - Instituto de Aeronática e Espaço, São José dos Campos, SP, Brazil
marciomtm@fab.mil.br

Abstract. *Understanding the development of hydrodynamic instability in a free shear layer compose of two different chemical species is of utmost importance in aerospace propulsion for the development of more effective combustors. The differences between physical properties of each species, in special the density stratification in the presence of the gravity force, may influence the characteristic of the flow, affecting the growth rate of the disturbances and the flow topology. The present study considers the temporal stability of mixing layers using direct numeric simulation and compares results with results from the bibliography. The simulations show a damping effect of the growth rate with increasing compressibility and viscous effects, confirming previous results available in the literature. The effect of body forces due to density gradients is investigated and the results show that for the cases considered in this study there may be a stabilization of the mixing layer with a reduction of the order of 30% for low values of the Froude number.*

Keywords: *Kelvin-Helmholtz instability, binary compressible mixing layer, Direct Numeric Simulation, Buoyancy Forces*

1. INTRODUCTION

The physical phenomena of mixing layer can be observed in nature, from clouds in the sky to river estuaries. In engineering, mixing layers composed of different chemical species are found in diffusion flames in combustion devices. The combustion efficiency can be measured by the amount of propellant that was burned, and this amount in a diffusion flame is proportional to the area of the flame, by studying means to better mix distinct species one can understand ways to increase the mixture and therefore improve the efficiency of the propulsive system. Except for some specific space applications, the combustion systems are under the influence of at least one body force, the gravity, and since the reactants have significant differences in density, buoyancy force effects are expected to be relevant. The present investigation uses direct numerical simulation to study how the compressibility, the variation of the physical properties due to the binary composition and the body forces affect the Kelvin-Helmholtz instability.

The study of the stability of binary mixing layer has already been addressed for example by Shin (2011), Mendonca (2014) and Salemi and Mendonca (2008) using linear stability analysis, and experimentally by the Brown and Roshko (1974), among others. More complex cases of binary mixing layers modified by jets and wakes have been studied by Soares *et al.* (2014), and Manco *et al.* (2015) also using linear stability analysis. Direct numerical simulation for homogeneous mixing layers has been used for example by Sandham and Reynolds (1991) and Quirino (2006) using the same methodology of the present work.

The effect of the compressibility in conjunction with the stratification of the density in a binary mixing layer has also been studied by Metcalfe *et al.* (1987) and by Fedioun and Lardjane (2005), both making an analysis of a temporally growing mixing layer, and the work of Kozusko *et al.* (1996), with a two-dimensional spatial analysis using the linear stability theory.

Regarding the analysis of body forces effect on the stability, the topic is more recent and have been studied by Lawson (2005), with a temporal, spatial, linear stability analysis of a jet. Also an experimental study was performed by Atsavapranee and Gharib (1997) to see the structures in a stratified plane mixing layer using a tilting tank. They discuss the effect of the gravity on the stability problem.

The present investigation is concerned with the stability of a mixing layer composed of a stream of oxygen flowing over a stream of hydrogen. The flow regime is considered compressible in a sense that Mach numbers may be as high as transonic. Density variations are also a result of mass diffusion through the mixing layer. The formulation and numerical methods are discussed in the following section. Results are presented next, starting with a code verification for a homoge-

neous mixing layer. Results for the mixing layer stability with and without body forces are presented after the verification and conclusions are presented in the final section.

2. METHODOLOGY

The temporal evolution of Kelvin-Helmoltz instability in a compressible, binary mixing layer is investigated through the direct numerical solution of the continuity, momentum, energy and mass fraction species equations. The mixing layer composed of a stream of oxygen over a stream of hydrogen is considered two-dimensional with no chemical reaction. Body forces are taken into account due to the strong density gradient. The perfect gas relation is assumed for the equation of state and the chemical properties of each gas are given as a function of the mass fraction and temperature according to the Chapman-Enskog and Wassiljewa theories. This is a more precise way to calculate the physical properties of the mixture since, as can be seen in Kozusko *et al.* (1996), simplified forms lead to errors in the solution. The hydostatic force was disconsider in the avaliation of tha variation of the density. The equations are written in a non-dimensional form and the resulting non-dimensional numbers are varied in order to investigate different flow conditions. The equations and the reference scales are presented in the next section. The equations are discretized using high order, low dissipation and low dispersion methods.

2.1 Governing Equations

$$\frac{\partial \hat{\rho}}{\partial \hat{t}} + \frac{\partial}{\partial \hat{x}}(\hat{\rho}\hat{u}) + \frac{\partial}{\partial \hat{y}}(\hat{\rho}\hat{v}) = 0, \tag{1}$$

$$\frac{\partial}{\partial \hat{t}}(\hat{\rho}\hat{u}) + \frac{\partial}{\partial \hat{x}}(\hat{\rho}\hat{u}^2 + \hat{p} - \hat{\tau}_{xx}) + \frac{\partial}{\partial \hat{y}}(\hat{\rho}\hat{u}\hat{v} - \hat{\tau}_{xy}) = 0, \tag{2}$$

$$\frac{\partial}{\partial \hat{t}}(\hat{\rho}\hat{v}) + \frac{\partial}{\partial \hat{x}}(\hat{\rho}\hat{u}\hat{v} - \hat{\tau}_{xy}) + \frac{\partial}{\partial \hat{y}}(\hat{\rho}\hat{v}^2 + \hat{p} - \hat{\tau}_{yy}) - \hat{\rho}\hat{g}_y = 0, \tag{3}$$

$$\frac{\partial}{\partial \hat{t}}(\hat{E}_t) + \frac{\partial}{\partial \hat{x}}\left[(\hat{E}_t + \hat{p})\hat{u} + \hat{q}_x - \hat{u}\hat{\tau}_{xx} - \hat{v}\hat{\tau}_{xy}\right] + \frac{\partial}{\partial \hat{y}}\left[(\hat{E}_t + \hat{p})\hat{v} + \hat{q}_y - \hat{u}\hat{\tau}_{xy} - \hat{v}\hat{\tau}_{yy}\right] - \hat{\rho}\hat{v}\hat{g}_y = 0, \tag{4}$$

$$\frac{\partial}{\partial \hat{t}}(\hat{\rho}\hat{Y}_I) + \frac{\partial}{\partial \hat{x}}\left(\hat{\rho}\hat{u}\hat{Y}_I - \hat{\rho}\hat{D}\frac{\partial \hat{Y}_I}{\partial \hat{x}}\right) + \frac{\partial}{\partial \hat{y}}\left(\hat{\rho}\hat{v}\hat{Y}_I - \hat{\rho}\hat{D}\frac{\partial \hat{Y}_I}{\partial \hat{y}}\right) = 0, \tag{5}$$

where E_t is the total energy defined as:

$$\hat{E}_t = \hat{\rho}\left[\hat{e} + \frac{1}{2}(\hat{u}^2 + \hat{v}^2)\right], \tag{6}$$

Using index notation, the viscous stresses are related to the strain tensor linearly:

$$\hat{\tau}_{ij} = -\frac{2}{3}\hat{\mu}\frac{\partial \hat{u}_k}{\partial \hat{x}_k}\delta_{ij} + \hat{\mu}\left(\frac{\partial \hat{u}_i}{\partial \hat{x}_j} + \frac{\partial \hat{u}_j}{\partial \hat{x}_i}\right), \tag{7}$$

and the heat diffusion is expressed according to the Fourier's law:

$$\hat{q}_i = \hat{k}\frac{\partial \hat{T}}{\partial \hat{x}_i}. \tag{8}$$

the notation $\hat{}$ denotes a dimensional variable.

The reference conditions used for the non-dimensional equations are the ones at the upper stream containing oxygen, except the characteristic length, $\hat{\delta}_w$ that is given by the mixing layer vorticity thickness, and $\hat{g}$ for the gravity. The resulting non-dimensional numbers are the Reynolds number, Re, the Prandlt number, Pr, the Lewis number, Le, the Mach number, Ma, and the Froude number, Fr, all defined below:

$$Re = \frac{\hat{\rho}_1\hat{U}_1\hat{\delta}_w}{\hat{\mu}_1}, \qquad Pr = \frac{\hat{\mu}_1\hat{c}_{p_1}}{\hat{k}_1}, \qquad Ma = \frac{\hat{U}_1}{\hat{a}_1}, \qquad Le = \frac{\hat{k}_1}{\hat{\rho}_1\hat{D}\hat{c}_{p_1}}, \qquad Fr = \frac{\hat{U}_1}{\sqrt{\hat{\delta}_w\hat{g}}}, \tag{9}$$

where, ρ is the density, u and v are the velocities parallel and normal to the free stream direction, p is pressure, q is heat conduction, D is the mass diffusion coefficient, Y_1 is the mass fraction of the oxygen, e is the internal energy. The ρ_1, U_1, μ_1, k_1, c_{p_1} and a_1 are respectively the density, free stream velocity, dynamic viscosity, thermal conductivity, specific

heat at constant pressure and speed of sound, all defined at the upper free stream, indicated by the subscript 1. With this the equations can be written in a non-dimensional form:

$$\frac{\partial \rho}{\partial t} + \frac{\partial}{\partial x}(\rho u) + \frac{\partial}{\partial y}(\rho v) = 0 \tag{10}$$

$$\frac{\partial}{\partial t}(\rho u) + \frac{\partial}{\partial x}(\rho u^2 + p - \frac{1}{Re_1}\tau_{xx}) + \frac{\partial}{\partial y}(\rho uv - \frac{1}{Re_1}\tau_{xy}) = 0 \tag{11}$$

$$\frac{\partial}{\partial t}(\rho v) + \frac{\partial}{\partial x}(\rho uv - \frac{1}{Re_1}\tau_{xy}) + \frac{\partial}{\partial y}(\rho v^2 + p - \frac{1}{Re_1}\tau_{yy}) - \frac{\rho}{Fr^2} = 0 \tag{12}$$

$$\frac{\partial}{\partial t}(E_t) + \frac{\partial}{\partial x}\left[(E_t + p)u + \frac{q_x}{Ma_1^2(\gamma-1)Re_1 Pr_1} - \frac{1}{Re_1}\tau_{xx} - \frac{1}{Re_1}\tau_{xy}\right] + \frac{\partial}{\partial y}\left[(E_t + p)v + \frac{q_y}{Ma_1^2(\gamma-1)Re_1 Pr_1} - \frac{1}{Re_1}\tau_{xy} - \frac{1}{Re_1}\tau_{yy}\right] - \frac{\rho v}{Fr^2} = 0 \tag{13}$$

$$\frac{\partial}{\partial t}(\rho Y_I) + \frac{\partial}{\partial x}\left(\rho u Y_I - \frac{1}{Re_1 Pr_1 Le_1}\rho D\frac{\partial Y_I}{\partial x}\right) + \frac{\partial}{\partial y}\left(\rho v Y_I - \frac{1}{Re_1 Pr_1 Le_1}\rho D\frac{\partial Y_I}{\partial y}\right) = 0 \tag{14}$$

2.2 Numerical Methodology

Since the perturbations are a small deviations from a base flow, its necessary to use high order numerical schemes, with low dissipation and dispersion properties. Therefore, for spatial and temporal discretization the following schemes are used in the code: (i) spatial schemes, 4th order central finite difference, (ii) temporal schemes, 4th order, 4 steps Runge Kutta.

For the boundary conditions of the numeric domain, periodic conditions in the left and right boundaries are use and for the upper and lower boundaries the gradient in the normal direction of all variables is forced to be zero.

For all the test cases the initial conditions are set as a base flow plus a small perturbation in the velocity field. The base flow is assumed parallel and the velocity distribution follows a hyperbolic tangent profile given by Eq. 15.

$$U(y) = \frac{1}{2}\left[(U_1 + U_2) + (U_1 - U_2)\tanh\left(\frac{2y}{\delta_w}\right)\right] \tag{15}$$

Where U_2 is the lower free stream speed.

For the binary cases a initial mass fraction profile was used also following a hyperbolic tangent given by Eq. 16.

$$Y_1(y) = \frac{1}{2}\left[1 + \tanh\left(\frac{2y}{\delta_w}\right)\right] \tag{16}$$

The initial temperature is considered constant throughout the domain at the initial condition. The density varies according to the mass fraction distribution and the pressure is computed using the perfect gas relation.

The upper free stream has non-dimensional velocity $U_1 = 1$ and the lower free stream is chosen to have velocity $U_2 = -1$. To obtain the thermodynamic properties for the species it is necessary to give a reference dimensional temperature, so $T_{ref} = 273.15$ K was used.

3. RESULTS

3.1 Code Verification - The homogeneous case

The present DNS code for binary mixing layers was adapted from the homogeneous code developed by Quirino (2006) by adding the species conservation equation and different relations to calculate the mixture and the species properties.

In order to do a code verification, the gas properties were considered constant over the domain in order to simulate a homogeneous mixing layer and the results were compared with Sandham (1990). Sandham's data was obtained from an inviscid linear stability theory code, while the present formulation take the viscous terms into consideration. Therefore, a large Reynolds number is used to accomplish a better agreement. Figure 1 shows the growth rate ω_i versus wavenumber α for $Ma = 0.4$ and $Re = 20,000$. Growth rates are measured as the amplification of the maximum normal velocity component.

Table 1 shows the percentage difference between the present results and results from Sandham (1990) for two different Reynolds Numbers. Sandham considered inviscid simulations and the present results show better agreement for $Re = 20,000$, where viscous effects are lower. The difference between the present results and Sandham's results is of the order of 1% or lower.

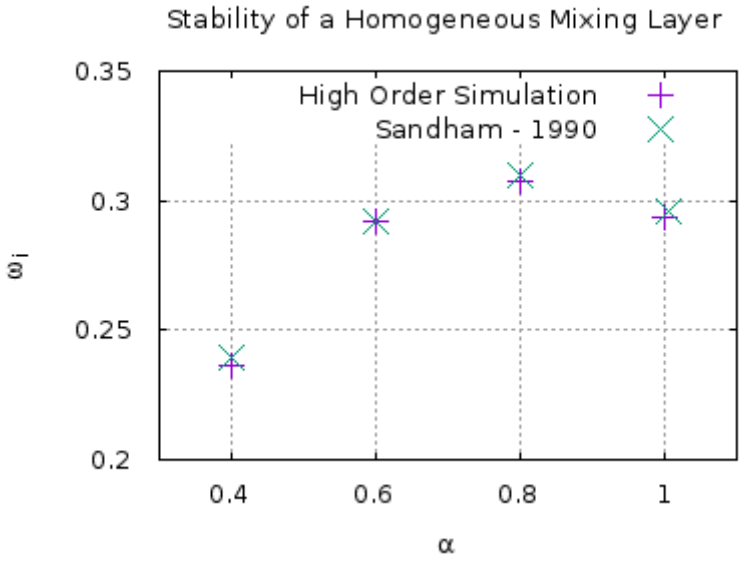

Figure 1. Growth rate versus wavenumber for a homogeneous mixing layer. Comparison between direct numerical simulation and linear stability theory results.

Table 1. Growth rate results for different wavenumber. Differences between the simulation and the literature

Wavenumber	Re = 5,000	Re = 20,000	(Sandham, 1990)	Error$^{(1)}$ (%)	Error$^{(2)}$ (%)
0.4	0.234979	0.236610	0.239087	1.718	1.036
0.6	0.286207	0.292135	0.291754	1.901	0.130
0.8	0.298040	0.307599	0.309421	3.678	0.589
1.0	0.281456	0.293292	0.295843	4.863	0.862

$^{(1)}$ for the Re = 5,000
$^{(2)}$ for the Re = 20,000

3.2 Binary Mixing Layer Results - without buoyancy

Table 2 shows the comparison between the binary case and the homogeneous case at a Reynolds number of $Re = 20,000$, and a Mach number of $Ma = 0.4$. The binary mixing layer has a lower growth rate than the homogeneous case for all wavenumber tested, showing that the binary mixing produces a damping effect on the stability of the Kelvin-Helmholtz structures. This stabilization effect can also be seen on the pressure and the vorticity fields as seen in Figs. 2 and 3 for $\alpha = 0.8$, which is the wavenumber that gives the highest growth rate for the homogeneous case.

Table 2. Growth rate difference between the binary case and the homogeneous case as a function of the wavenumber.

Wavenumber	Binary$^{(1)}$	Homogeneous$^{(1)}$	Reduction (%)
0.4	0.131673	0.236610	44.35
0.6	0.161122	0.292135	44.58
0.8	0.170984	0.307599	44.13
1.0	0.160892	0.293292	45.36

$^{(1)}$ for the $Re = 20,000$ and $Ma = 0.4$

A linear stability analysis based on the Rayleigh equation for a binary mixing layer (based on the solver by Salemi and Mendonca (2008)) was also performed and the results are shown in Figs. 4 and 5. Figure 4 show the effect of compressibility on a homogeneous mixing layer. Increasing the Mach number from 0.2 to 0.4 and 0.8 show that the maximum amplification rate as well as the range of unstable wavenumbers is reduced.

Results are also presented for a fixed Mach number equal to 0.4, and density ratios of 1, 0.06 and 16, corresponding to a homongeneous mixing layer, a H2/O2 mixing layer (H2 on the upper stream) and a O2/H2 mixing layer. The results show that the binary mixing layer is more stable than the homogeneous one, both in terms of the growth rates and range of unstable wavenumbers. Without taking into account body forces, when the lighter fluid is on top the mixing layer is the most stable. This is due to the distributions of $U(y)$ and $\rho(y)$ used in the stability analysis. It is also interesting to note

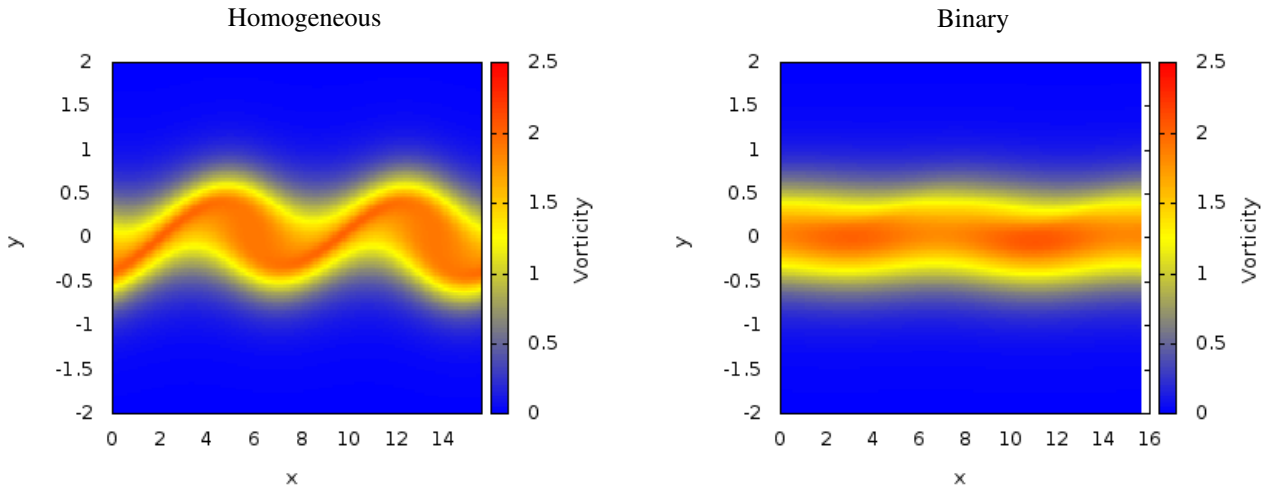

Figure 2. Vorticity distribution, comparison between homogeneous and binary mixing layers.

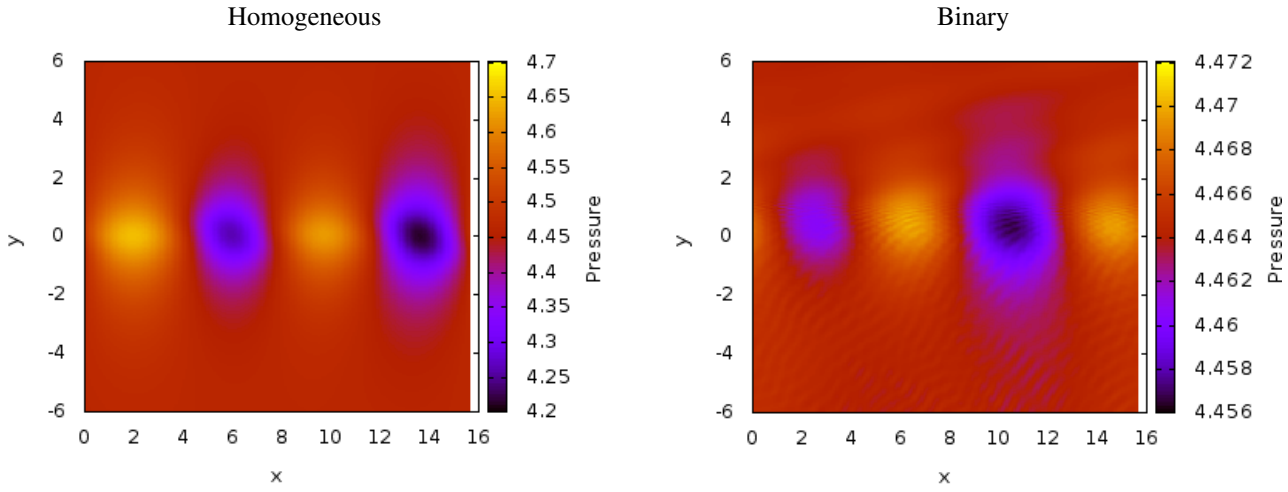

Figure 3. Pressure distribution, comparison between homogeneous and binary mixing layers.

that the wavenumber corresponding to the larges growth rate changes both with Mach number and density ratio.

3.3 Binary Mixing Layer Under the Effect of Buoyancy Forces.

The effect of gravity forces are represented by the Froude number, which is a ratio between inertia and body forces. For large Froude numbers the body forces become negligible and the stability results tend to the results obtained in the previous section.

A range of Froude number were simulated from a low value of 30 to a high value of 3,000. This range was simulated for two different of compressibility levels, $Ma = 0.4$ and $Ma = 0.8$, and inertia, $Re = 20,000$ and $Re = 2,000$. Since the simulations have a long time of convergence, only one wavenumber was tested, the one with the largest amplification rate in the previous section, $\alpha = 0.8$. Considering the typical values of O2 and H2 properties, Mach numbers up to transonic and Reynolds numbers on a range from 100 to 10,000, the order of magnitude of the Froude number is in the range of 3 to 30,000, showing that body forces effects may be relevant.

The results are presented in Tabs. 3 and 4. For a better clarity the tables compare two different Mach numbers for a fixed Reynolds number, in order to highlight the effect of compressibility. Table 3 maintain the $Re = 20,000$, in the attempt to simulate a inviscid case as show in section 3.2. It shows a comparison of the amplification rate for $Ma = 0.8$ and $Ma = 0.4$. It's possible to see that, as expected, when Froude is increased, the temporal growth rate ω_i tends to the value of the simulation without considering the body forces, with a difference between them of less than 0,5 %.

The results also show that the compressibility have a damping effect, reducing the growth of the perturbation when a higher Mach number is tested. The same behavior can be seen in the table 4, where the same parameters are tested but with a Reynolds number in a more viscous regime, as shows in section 3.2. The strong stabilizing effect of compressibility has already been shown in the literature, from linear stability theory and in experimental tests. The present results show that the compressibility effect is maintained even in the presence of body forces and viscosity. Comparing table 3 and 4

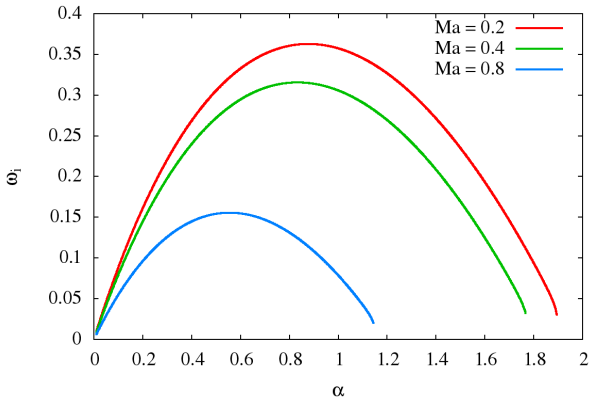

Figure 4. Growth rate for compressible mixing layer. Effect of compressibility. Homogeneous mixing layer.

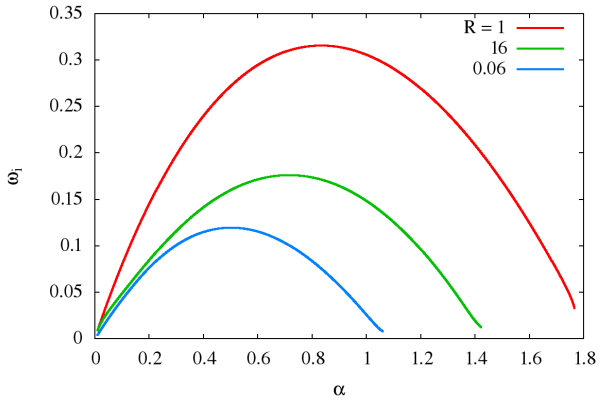

Figure 5. Growth rate for binary mixing layer. Effect of density stratification $R = \rho_1/\rho_2$. Mach $Ma = 0.4$.

shows that for every case the amplification rate is lower for the smaller Reynolds number, reinforcing that the viscosity have a stabilizer effect on the mixing layer.

Table 3. Difference of the growth rate as a function of the Froude number for two different Mach numbers and high Reynolds number. Wavenumber $\alpha = 0.8$.

Froude	$Ma = 0.4$	$Ma = 0.8$	Difference(%)
30	0.120300	0.112018	-7.39
100	0.155597	0.145981	-6.59
300	0.169329	0.151359	-11.87
1000	0.171465	0.152452	-12.42
3000	0.171649	0.152666	-12.43

for $Re = 20,000$

Table 4. Difference of the growth rate as a function of the Froude number for two different Mach numbers and considering higher viscous effects. Wavenumber $\alpha = 0.8$.

Froude	$Ma = 0.4$	$Ma = 0.8$	Difference(%)
30	0.107482	0.100266	-7.20
100	0.143003	0.134560	-6.27
300	0.149272	0.140741	-6.06
1000	0.150056	0.141517	-6.03
3000	0.150126	0.141585	-6.03

for $Re = 2,000$

At last, the results from tables 3 and 4 show the effect of body forces for wavenumber $\alpha = 0.8$. Both $Re = 20,000$ and $Re = 2,000$ show that, as the Froude number is reduced the growth rate is also reduced, showing that the density stratification have a stabilizing effect in the tested cases. For the higher Reynolds number and $Ma = 0.4$, when the Froude number is reduced from 3,000 to 30 the growth rate reduces by 30%, while for the lower Reynolds number the growth rate reduces by 28%. For the higher Mach number case, reducing the Froude number from 3,000 to 30 results in 27% and 29%, for Reynolds 20,000 and 2,000 respectively. The effect of body forces are more significant below Froude number equal to 300.

The results presented above may be summarized in Fig. 6, where the amplification rate is presented as a function of the Froude number for different values of Mach and Reynolds numbers. The amplification rate reaches a plateau above $Fr = 300$. Only the case Reynolds 20,000 and Mach number 0.4 show a more significant increase between Froude numbers of 100 to 300.

4. CONCLUSIONS

The present investigation shows results comparing the development of Kelvin-Helmholtz instabilities on homogeneous and a binary mixing layer composed of oxygen and hydrogen. The results show that the binary mixing layer is more stable

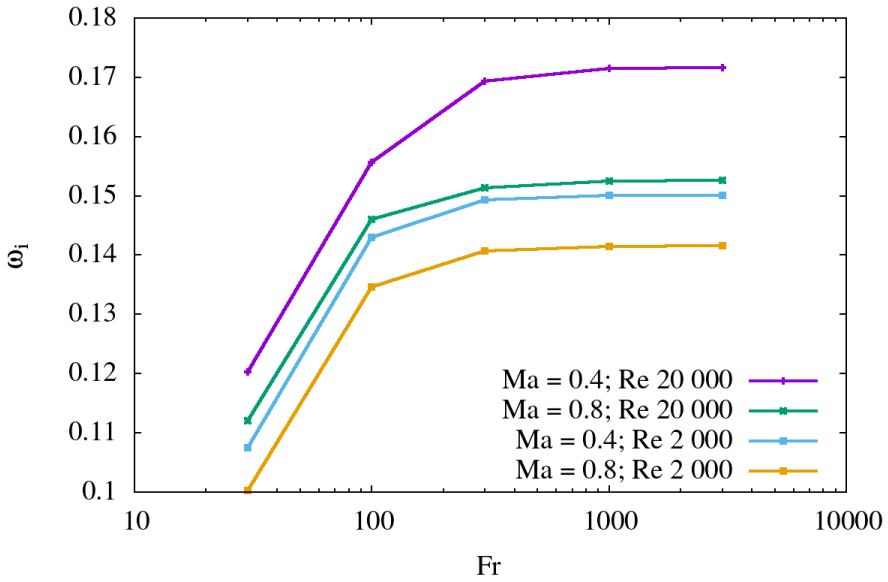

Figure 6. Amplification rate versus Froude number for different values of Ma and Re.

than the homogeneous one. As viscous effects and compressibility is increased the mixing layer becomes more stable, as already reported in the literature.

The effect of body forces due to strong gradients of density associated with the presence of different chemical species in the mixing layer shows that gravity has a stabilizing effect up to the order of 30% for the conditions tested in this investigation. The effect of body forces ceases to be relevant for Frounde numbers greater the 300.

5. ACKNOWLEDGEMENTS

The authors acknowledge the financial support of CAPES, under the grant 800012/2016-0, and support of CNPq, under the grants 302717/2016-1 and PVE-401032/2014-0.

6. REFERENCES

Atsavapranee, P. and Gharib, M., 1997. "Structures in stratified plane mixing layers and the effects of cross-shear". *Journal of Fluid Mechanics*, Vol. 342, p. 53âĂŞ86. doi:10.1017/S0022112097005399.

Brown, G.L. and Roshko, A., 1974. "On density effects and large structure in turbulent mixing layers". *Journal of Fluid Mechanics*, Vol. 64, pp. 775–781.

Fedioun, I. and Lardjane, N., 2005. "Temporal linear stability analysis of three- dimensional compressible binary shear layers". *AIAA Journal*, Vol. 43, No. 1, pp. 111–123.

Kozusko, F., Lasseigne, D.G., Grosch, C.E. and Jackson, T.L., 1996. "The stability of compressible mixing layers in binary gases". *Physics of Fluids*, Vol. 8, No. 7, pp. 1954–1963. doi:10.1063/1.868974. URL `https://doi.org/10.1063/1.868974`.

Lawson, Anthony L.; Parthasarathy, R.N., 2005. "Linear stability analysis of gravitational effects on a low-density gas jet injected into a high-density medium". Technical report, NASA.

Manco, J.A.A., Freitas, R.B., Fernandes, L.M. and Mendonca, M.T., 2015. "Stability of compressible mixing layers modified by wakes and jets". In *Procedia IUTAM, Vol 14, IUTAM Symp. on Laminar-Turbulent Transition*. Rio de Janeiro, Brazil, pp. 129–136.

Mendonca, M.T., 2014. "Linear stability analysis of binary compressible mixing layers modified by a jet or a wake deficit". In *52nd AIAA Aerospace Sciences Meeting and Exhibit*. National Harbor, Maryland, pp. 1–13.

Metcalfe, R.W., Orszag, S.A., Brachet, M.E., Menon, S. and Riley, J.J., 1987. "Secondary instability of a temporally growing mixing layer". *Journal of Fluid Mechanics*, Vol. 184, p. 207âĂŞ243. doi:10.1017/S0022112087002866.

Quirino, S.F., 2006. *Simulação numérica direta de camada cisalhante compressível com fonte de calor*. Dissertação (mestrado em engenharia e tecnologia espaciais), Instituto Nacional de Pesquisas Espaciais (INPE), São José dos Campos. INPE-14661-TDI/1217.

Salemi, L. and Mendonca, M.T., 2008. "Spatial and temporal linear stability analysis of binary compressible shear layer". In *AIAA 38th Fluid Dynamics Conference*. Seattle, USA, AIAA paper 2008-3841, pp. 1–23.

Sandham, N.D., 1990. *A Numerical Investigation of the Compressible Mixing Layer*. Ph.D. thesis, Stanfor University,

USA.

Sandham, N.D. and Reynolds, W.C., 1991. "Three-dimensional simulations of large eddies in the compressible mixing layer". *J. Fluid Mechanics*, Vol. **224**, pp. 133–158.

Shin, D.S., 2011. "Stability analysis of reacting mixing layers with density gradient and wake deficit". *Journal of Mechanical Science and Technology*, Vol. **25**, No. 3, pp. 683–688.

Soares, M.S., Filho, F.F. and Mendonça, M.T., 2014. "Effect of thickness ratio on the stability of mixing layers with a wake component". In *IX Escola de Primavera de Transição e Turbulência*. São Leopoldo, RS, pp. 1–7.

7. RESPONSIBILITY NOTICE

The authors are the only responsible for the printed material included in this paper.